Far-from-equilibrium dynamics with broken symmetries from the 1/N expansion of the 2PI effective action

Gert Aarts,[1,*] Daria Ahrensmeier,[2,†] Rudolf Baier,[2,‡] Jürgen Berges,[3,§] and Julien Serreau[3,‖]
[1]*Department of Physics, The Ohio State University, 174 West 18th Avenue, Columbus, Ohio 43210*
[2]*Fakultät für Physik, Universität Bielefeld, Universitätsstraße, 33615 Bielefeld, Germany*
[3]*Universität Heidelberg, Institut für Theoretische Physik, Philosophenweg 16, 69120 Heidelberg, Germany*
(Received 6 February 2002; published 15 August 2002)

We derive the nonequilibrium real-time evolution of an $O(N)$-invariant scalar quantum field theory in the presence of a nonvanishing expectation value of the quantum field. Using a systematic 1/N expansion of the 2PI effective action to next-to-leading order, we obtain nonperturbative evolution equations which include scattering and memory effects. The equivalence of the direct method, which requires the resummation of an infinite number of skeleton diagrams, with the auxiliary-field formalism, which involves only one diagram at next-to-leading order, is shown.

DOI: 10.1103/PhysRevD.66.045008 PACS number(s): 11.15.Pg, 05.70.Ln, 11.30.Qc

I. INTRODUCTION

Nonequilibrium quantum field theory has a wide range of applications, including current and upcoming relativistic heavy-ion collision experiments at the BNL Relativistic Heavy Ion Collider (RHIC) and CERN Large Hadron Collider (LHC), phase transitions in the early universe or the formation of Bose-Einstein condensates in the laboratory. Important theoretical progress has been achieved with effective descriptions based on a separation of scales in the weak-coupling limit [1], or for systems close to equilibrium using approximations such as (non)linear response or gradient expansions [2]. However, the description of far-from-equilibrium dynamics is still in its infancies. The situation is complicated by the fact that typically there is no clear separation of scales which is valid at all times and it is often difficult to identify a small expansion parameter. For example, standard perturbation theory is plagued by the problem that a secular (unbounded) time evolution prevents the description of the late-time behavior of quantum fields.

Practicable nonperturbative approximation schemes may be based on the two-particle irreducible (2PI) generating functional for Green's functions [3]. Recently, a systematic 1/N expansion of the 2PI effective action has been proposed and applied to a scalar $O(N)$-symmetric quantum field theory [4]. The approach provides a controlled nonperturbative description of far-from-equilibrium dynamics at early times as well as the late-time approach to thermal equilibrium and can be applied in extreme nonequilibrium situations [4,5]. This is in contrast with the standard 1/N expansion of the 1PI effective action which is secular in time once direct scattering is taken into account [6]. The 1/N expansion of the 2PI effective action extends previous successful descriptions of the large-time behavior of quantum fields [7,8], which employ the loop expansion of the 2PI effective action relevant at weak couplings [3,9,10]. For systems in or close to equilibrium recent applications of the loop expansion can be found in Refs. [11–14]. A 1/N expansion has the advantage over the loop expansion that it is not restricted to small couplings, an observation made in the context of nonequilibrium quantum field dynamics already for quite some time [15]. However, in order to describe quantum scattering and thermalization the inclusion of the usually discarded next-to-leading order (NLO) contributions is crucial.

In Ref. [4] the 1/N expansion of the 2PI effective action has been carried out to NLO in the symmetric regime for a vanishing expectation value ϕ of the quantum field. Here, we derive the evolution equations from the NLO approximation of the 2PI effective action for nonzero ϕ. A nonvanishing field expectation value is important to describe the physics of heavy ion collisions, where the presence of a substantial scalar quark-antiquark condensate signals the spontaneous breakdown of chiral symmetry. [In the language of the $O(4)$ linear sigma model for two-flavor QCD one has $\phi \sim \langle \bar{q} q \rangle$.] Important nonequilibrium applications in this context include the formation of disoriented chiral condensates (DCCs, cf. [16]) or the decay [17] of parity odd metastable states in hot QCD [18]. Similar far-from-equilibrium applications in inflationary cosmology concern the phenomenon of preheating, where the dynamics of the inflaton ϕ is expected to trigger explosive particle production (see, e.g., [19]). The availability of a quantum field description of the dynamics is important for cases where the effectively classical approximation (in the context of inflation, see e.g. [20]) may not be appropriate.

In this work, we perform a systematic 1/N expansion of the 2PI effective action to next-to-leading order. A detailed discussion of the classification of diagrams is given in Sec. III. This allows us to give the effective action (Sec. IV) and the equations of motion (Sec. V) in a straightforward manner. In Sec. VI it is shown how this result is obtained using the auxiliary-field formalism [21]. The causal equations for the spectral and statistical functions are listed in Sec. VII and

*Email address: aarts@mps.ohio-state.edu
†Email address: dahrens@physik.uni-bielefeld.de
‡Email address: baier@physik.uni-bielefeld.de
§Email address: j.berges@thphys.uni-heidelberg.de
‖Email address: serreau@thphys.uni-heidelberg.de

a perturbative approximation to second order in the coupling constant is given in Sec. VIII. In two Appendixes we discuss further features of the equations and the realization of Goldstone's theorem.

II. THE 2PI EFFECTIVE ACTION

We consider a real scalar N-component quantum field φ_a $(a=1,\ldots,N)$ with a classical $O(N)$-invariant action

$$S[\varphi]=\int d^{d+1}x\left[\frac{1}{2}\partial_{x^0}\varphi_a\partial_{x^0}\varphi_a-\frac{1}{2}\partial_{\mathbf{x}}\varphi_a\partial_{\mathbf{x}}\varphi_a-\frac{1}{2}m^2\varphi_a\varphi_a-\frac{\lambda}{4!N}(\varphi_a\varphi_a)^2\right]. \tag{1}$$

Summation over repeated indices is implied and $x\equiv(x^0,\mathbf{x})$. All correlation functions of the quantum theory can be obtained from the effective action $\Gamma[\phi,G]$, the two-particle irreducible (2PI) generating functional for Green's functions parametrized by the macroscopic field $\phi_a(x)$ and the composite field $G_{ab}(x,y)$, given by

$$\phi_a(x)=\langle\varphi_a(x)\rangle, \tag{2}$$

$$G_{ab}(x,y)=\langle T_{\mathcal{C}}\varphi_a(x)\varphi_b(y)\rangle-\langle\varphi_a(x)\rangle\langle\varphi_b(y)\rangle. \tag{3}$$

The brackets denote the expectation value with respect to the density matrix and $T_{\mathcal{C}}$ denotes time-ordering along a contour $\mathcal{C}$ in the complex time plane. At this stage the explicit form of the contour is not needed.

A discussion of the defining functional integral of the 2PI effective action can be found in Ref. [3]. Following [3] it is convenient to parametrize the 2PI effective action as

$$\Gamma[\phi,G]=S[\phi]+\frac{i}{2}\mathrm{Tr}\ln G^{-1}+\frac{i}{2}\mathrm{Tr}\,G_0^{-1}(\phi)G+\Gamma_2[\phi,G]+\text{const.} \tag{4}$$

Here the classical inverse propagator $iG_0^{-1}(\phi)$ is given by

$$iG^{-1}_{0,ab}(x,y;\phi)\equiv\frac{\delta^2S[\phi]}{\delta\phi_a(x)\,\delta\phi_b(y)}=-\left(\left[\Box_x+m^2+\frac{\lambda}{6N}\phi^2(x)\right]\delta_{ab}+\frac{\lambda}{3N}\phi_a(x)\phi_b(x)\right)\delta_{\mathcal{C}}(x-y) \tag{5}$$

with $\phi^2\equiv\phi_a\phi_a$ and $\delta_{\mathcal{C}}(x-y)\equiv\delta_{\mathcal{C}}(x^0-y^0)\,\delta^d(\mathbf{x}-\mathbf{y})$. The contribution $\Gamma_2[\phi,G]$ is given by all closed 2PI graphs[1] with the propagator lines set equal to G [3]. The effective interaction vertices are obtained from the terms cubic and higher in φ in the classical action (1) after shifting the field $\varphi\to\phi+\varphi$. In presence of the nonvanishing expectation value ϕ this results in a cubic and a quartic vertex

$$\mathcal{L}_{\mathrm{int}}(x;\phi,\varphi)=-\frac{\lambda}{6N}\phi_a(x)\varphi_a(x)\varphi_b(x)\varphi_b(x)-\frac{\lambda}{4!N}[\varphi_a(x)\varphi_a(x)]^2. \tag{6}$$

Dynamical equations for ϕ_a and G_{ab} can be found by minimizing the effective action. In the absence of external sources physical solutions require

$$\frac{\delta\Gamma[\phi,G]}{\delta\phi_a(x)}=0, \tag{7}$$

which leads to the macroscopic field evolution equation

$$-\left(\Box_x+m^2+\frac{\lambda}{6N}[\phi^2(x)+G_{bb}(x,x)]\right)\phi_a(x)=\frac{\lambda}{3N}\phi_b(x)G_{ba}(x,x)-\frac{\delta\Gamma_2[\phi,G]}{\delta\phi_a(x)}, \tag{8}$$

as well as

$$\frac{\delta\Gamma[\phi,G]}{\delta G_{ab}(x,y)}=0, \tag{9}$$

which leads to

$$G^{-1}_{ab}(x,y)=G^{-1}_{0,ab}(x,y)-\Sigma_{ab}(x,y;\phi,G) \tag{10}$$

with

$$\Sigma_{ab}(x,y;\phi,G)\equiv 2i\frac{\delta\Gamma_2[\phi,G]}{\delta G_{ab}(x,y)}. \tag{11}$$

Equation (10) can be rewritten as a partial differential equation suitable for initial value problems by convolution with G,

[1] A graph is two-particle irreducible if it does not become disconnected upon opening two propagator lines.

$$\int_z G^{-1}_{0,ab}(x,z)G_{bc}(z,y)$$

$$= \int_z \Sigma_{ac}(x,z)G_{cb}(z,y) + \delta_{ab}\delta_{\mathcal{C}}(x-y), \quad (12)$$

where the shorthand notation $\int_z = \int_{\mathcal{C}} dz^0 \int d\mathbf{z}$ is employed. With the classical inverse propagator (5) this differential equation reads explicitly

$$-\left[\Box_x + m^2 + \frac{\lambda}{6N}\phi^2(x)\right]G_{ab}(x,y)$$

$$= \frac{\lambda}{3N}\phi_a(x)\phi_c(x)G_{cb}(x,y)$$

$$+ i\int_z \Sigma_{ac}(x,z;\phi,G)G_{cb}(z,y) + i\,\delta_{ab}\delta_{\mathcal{C}}(x-y). \quad (13)$$

The evolution of ϕ_a and G_{ab} is determined by Eqs. (8) and (13), once $\Gamma_2[\phi,G]$ is specified.

III. THE 1/*N* EXPANSION OF THE 2PI EFFECTIVE ACTION

In this section we discuss the $1/N$ expansion of the 2PI effective action proposed in Ref. [4] in more detail. We present a simple classification scheme based on $O(N)$ invariants which parametrize the 2PI diagrams contributing to $\Gamma[\phi,G]$. The effective action at a given order in $1/N$ can then be obtained from a straightforward summation of the diagrams contributing at that order. The NLO result for $\Gamma[\phi,G]$ for general field configurations (ϕ, G) is presented in Sec. IV. Below we will compare the direct summation procedure described here with an alternative method, which employs an auxiliary field to simplify the summation (cf. Sec. VI).

A. Counting rules for irreducible $O(N)$ invariants

Following standard procedures [22] the interaction term of the classical action in Eq. (1) is written such that $S[\phi]$ scales proportional to N. From the fields ϕ_a alone one can construct only one independent invariant under $O(N)$ rotations, which can be taken as $\mathrm{tr}\,\phi\phi \equiv \phi^2 = \phi_a\phi_a \sim N$. The minimum ϕ_0 of the classical effective potential for this theory is given by $\phi_0^2 = N(-6m^2/\lambda)$ for negative mass-squared m^2 and scales proportional to N. Similarly, the trace with respect to the field indices of the classical propagator G_0 is of order N.

The 2PI effective action is a singlet under $O(N)$ rotations and parametrized by the two fields ϕ_a and G_{ab}. To write down the possible $O(N)$ invariants, which can be constructed from these fields, we note that the number of ϕ fields has to be even in order to construct an $O(N)$ singlet. For a compact notation we use $(\phi\phi)_{ab} = \phi_a\phi_b$. Consider a general singlet composed of arbitrary powers of $(\phi\phi)_{ab}$ and G_{ab} (we neglect all space-time dependencies)

$$s = \mathrm{tr}[(\phi\phi)^{p_1}G^{q_1}\cdots(\phi\phi)^{p_n}G^{q_n}]$$

$$= (\phi^2)^{p_1+\cdots+p_n-n}\mathrm{tr}(\phi\phi\,G^{q_1})\cdots\mathrm{tr}(\phi\phi\,G^{q_n}) \quad (14)$$

for $p_i \neq 0$, where the p_i and q_i $(i=1,\ldots,n)$ are any positive integer. [For all $p_i = 0$ the right-hand side (RHS) is given by $\mathrm{tr}\,G^{q_1+\cdots+q_n}$.] The second line in the above equation follows from simple contraction of the field indices and corresponds to the fact that all functions of ϕ and G, which are singlets under $O(N)$, can be built from the irreducible (i.e. nonfactorizable in field-index space) invariants

$$\phi^2, \quad \mathrm{tr}(G^n) \quad \text{and} \quad \mathrm{tr}(\phi\phi G^n). \quad (15)$$

We note that for given N only the invariants with $n \leqslant N$ are irreducible. However, we will see below that for lower orders in $1/N$ and for sufficiently large N one has $n < N$. In particular, for the next-to-leading order approximation one finds that only invariants with $n \leqslant 2$ appear.

Since each single graph contributing to $\Gamma[\phi,G]$ is an $O(N)$ singlet, we can express them with the help of the set of invariants in Eq. (15). The factors of N in a given graph have two origins: each irreducible invariant is taken to scale proportional to N since it contains exactly one trace over the field indices, while each vertex provides a factor of $1/N$. The leading order (LO) graphs then scale proportional to N (as the classical action S), next-to-leading order (NLO) contributions are of order one, the next-to-next-to-leading order (NNLO) scales as $1/N$ and so on. This provides a well-defined expansion of $\Gamma[\phi,G]$ in powers of $1/N$. We stress that by construction each order in the $1/N$ expansion of the 2PI effective action respects $O(N)$ symmetry. In particular, this is crucial for the validity of Goldstone's theorem in the case of spontaneous symmetry breaking. For constant $\phi \neq 0$ one observes that the mass matrix $\sim \delta^2\Gamma[\phi,G^{(\mathrm{stat})}(\phi)]/\delta\phi_a\delta\phi_b$, with $G^{(\mathrm{stat})}(\phi)$ being the solution of Eq. (9), contains $(N-1)$ massless "transverse" modes and one massive "longitudinal" mode (see Appendix A for a discussion).

B. Classification of diagrams

In the following we will classify the various diagrams contributing to $\Gamma[\phi,G]$. The expression (4) for the 2PI effective action contains, besides the classical action, the one-loop contribution proportional to $\mathrm{Tr}\ln G^{-1} + \mathrm{Tr}\,G_0^{-1}(\phi)G$ and a nonvanishing $\Gamma_2[\phi,G]$ if higher loops are taken into account. The one-loop term contains both LO and NLO contributions. The logarithmic term corresponds, in absence of other terms, simply to the free field effective action and scales proportional to the number of field components N. To separate the LO and NLO contributions at the one-loop level consider the second term $\mathrm{Tr}\,G_0^{-1}(\phi)G$. From the form of the classical propagator (5) one observes that it can be decomposed into a term proportional to $\mathrm{tr}(G) \sim N$ and terms (neglecting all the space-time structure)

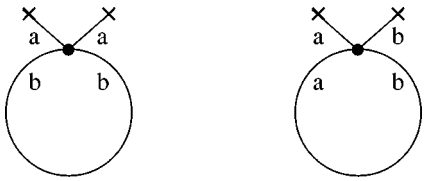

FIG. 1. Graphical representation of the ϕ-dependent contributions for $\Gamma_2 \equiv 0$. The crosses denote field insertions $\sim \phi_a \phi_a$ for the left figure, which contributes at leading order, and $\sim \phi_a \phi_b$ for the right figure contributing at next-to-leading order.

$$\sim \frac{\lambda}{6N}[\mathrm{tr}(\phi\phi)\mathrm{tr}(G) + 2\,\mathrm{tr}(\phi\phi G)]. \tag{16}$$

This can be seen as the sum of two "2PI one-loop graphs" with field insertion $\sim \phi_a \phi_a$ and $\sim \phi_a \phi_b$, respectively. Counting the factors of N coming from the traces and the prefactor, one observes that only the first of the two terms in Eq. (16) contributes at LO, while the second one is of order one (see Fig. 1).

We now turn to $\Gamma_2[\phi, G]$ which contains all 2PI diagrams beyond the one-loop level. The graphs are constructed from the three-point vertex and the four-point vertex in the interaction Lagrangian (6) with G associated to the propagator lines. From the three-vertex $\sim \phi_a$ one easily observes that one cannot construct a diagram which has a field insertion $\sim \phi^2 = \phi_a \phi_a$. As a consequence, all loop diagrams beyond the one-loop level can only depend on the basic invariants $\mathrm{tr}(G^n)$ and $\mathrm{tr}(\phi\phi G^n)$. Furthermore, we note that the invariant $\mathrm{tr}(G) = G_{aa}$ can only appear if the graph contains a tadpole as shown in Figs. 2 and 3. The first graph, Fig. 2, is proportional to the product of the term $[\mathrm{tr}(G)]^2$ and a factor $1/N$ from the quartic vertex. It therefore contributes at LO to the effective action. The graph in Fig. 3 is proportional to $\mathrm{tr}(G^2)/N$ and is of order one. The two-loop graphs shown in these figures are indeed the only two-particle irreducible graphs which contain a tadpole. As a consequence, the only invariants that can arise beyond two loops are $\mathrm{tr}(G^{n\geqslant 2})$ and $\mathrm{tr}(\phi\phi G^{n\geqslant 1})$.

Using these considerations, one can now straightforwardly continue to classify all the diagrams at a given order of the $1/N$ expansion. Consider a graph with V_3 three-point and V_4 four-point vertices. The number of internal lines I is determined by the familiar relation

$$2I = 3V_3 + 4V_4. \tag{17}$$

We observe again that V_3 has to be even. This graph contains $V_3/2$ field insertions $\sim \phi\phi$, $2V_4 + \frac{3}{2}V_3$ propagators G and

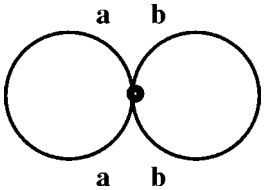

FIG. 2. LO contribution to the 2PI effective action.

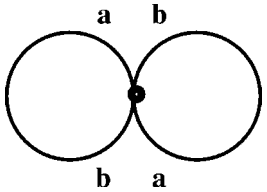

FIG. 3. NLO "double bubble" contribution.

comes with a factor $(\lambda/N)^{V_3+V_4}$ from the vertices. The highest power of N is obtained by contracting the ϕ and the G field such that the largest number of invariants $\mathrm{tr}(G^{n\geqslant 2})$ and $\mathrm{tr}(\phi\phi G^{n\geqslant 1})$ appears. The structure with the highest power of N,

$$\sim \left[\frac{\lambda}{N}\right]^{V_3+V_4} [\mathrm{tr}(\phi\phi G)]^{V_3/2} [\mathrm{tr}(G^2)]^{V_4+V_3/2}, \tag{18}$$

is of order one and contributes therefore at NLO.

For $V_3 = 0$ the corresponding diagrams are shown in Fig. 4 [4]. For $V_3 = 2$ the infinite series of graphs is presented in Fig. 5. We will now argue that graphs with $V_3 \geqslant 4$ are not two-particle irreducible such that we have classified the complete NLO contribution. We note that the invariant $\mathrm{tr}(\phi\phi G)$ connects the field insertion $\sim \phi_a \phi_b$ with a single propagator line. If a diagram contains that invariant more than once it is always possible to disconnect the graph by cutting two lines.[2] Consequently, a diagram with the above structure and with $V_3 \geqslant 4$ is not two-particle irreducible and does not contribute to $\Gamma[\phi, G]$. We therefore have classified all possible diagrams which contribute to the 2PI effective action at NLO and present the result in the next section. In Appendix A we discuss possible further approximations consistent with an expansion in powers of $1/N$.

IV. THE 2PI EFFECTIVE ACTION AT NLO

We write

$$\Gamma_2[\phi, G] = \Gamma_2^{\mathrm{LO}}[G] + \Gamma_2^{\mathrm{NLO}}[\phi, G] + \cdots \tag{20}$$

where Γ_2^{LO} denotes the leading order (LO) and Γ_2^{NLO} the next-to-leading order (NLO) contributions. The LO contribution to $\Gamma_2[G]$ is given by the diagram presented in Fig. 2,

[2]To see this, note that the number of loops L in these diagrams is given by the standard relation

$$L = I - V_3 - V_4 + 1 = V_4 + \frac{V_3}{2} + 1, \tag{19}$$

where we have used Eq. (17) for the second equality. Tadpole diagrams are forbidden in those graphs and each "bubble" $\mathrm{tr}(G^2)$ corresponds to one closed loop. From the above relation one then observes that the total number of loops in the diagram is given by the number of bubbles plus one. In particular, one can disconnect the diagram by cutting two lines connecting the fields insertions [the terms $\sim \mathrm{tr}(\phi\phi G)$].

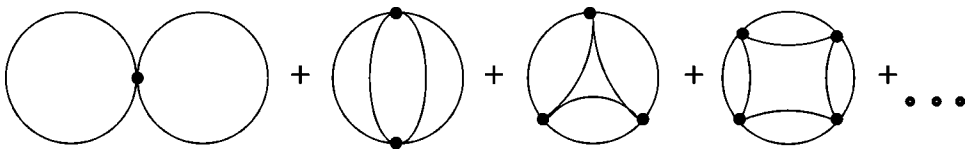

FIG. 4. NLO ϕ-independent contribution to the 2PI effective action. Higher loop diagrams in the infinite series can be obtained from the previous one by introducing another ''rung'' with two propagator lines at each vertex. The resummed series including the prefactors not displayed in the figure is given by the first term in Eq. (22).

$$\Gamma_2^{\mathrm{LO}}[G]=-\frac{\lambda}{4!N}\int_x G_{aa}(x,x)G_{bb}(x,x). \tag{21}$$

This contribution is ϕ independent.

The NLO contribution consists of an infinite series of diagrams which fall into two classes. The first class is independent of ϕ and is constructed with only quartic vertices. It contains the complete NLO contribution when $\phi=0$ and has been resummed in Ref. [4]. The diagrams are shown in Fig. 4. The second class depends on ϕ and contributes for the case of a nonzero field expectation value. This series of diagrams is shown in Fig. 5 and can be resummed as well. As a result, the NLO contribution to $\Gamma_2[\phi,G]$ is given by the sum of the two resummed expressions and reads[3]

$$\Gamma_2^{\mathrm{NLO}}[\phi,G]=\frac{i}{2}\mathrm{Tr}_{\mathcal{C}}\mathrm{Ln}[\mathbf{B}(G)]+\frac{i\lambda}{6N}\times\int_{xy}\mathbf{I}(x,y;G)\phi_a(x)G_{ab}(x,y)\phi_b(y). \tag{22}$$

In the above equation we have defined

$$\mathbf{B}(x,y;G)=\delta_{\mathcal{C}}(x-y)+i\frac{\lambda}{6N}G_{ab}(x,y)G_{ab}(x,y), \tag{23}$$

and the logarithm in Eq. (22) sums the infinite series shown in Fig. 4,

$$\mathrm{Tr}_{\mathcal{C}}\mathrm{Ln}[\mathbf{B}(G)]=\int_x\left(i\frac{\lambda}{6N}G_{ab}(x,x)G_{ab}(x,x)\right)-\frac{1}{2}\int_{xy}\left(i\frac{\lambda}{6N}G_{ab}(x,y)G_{ab}(x,y)\right)\times\left(i\frac{\lambda}{6N}G_{a'b'}(y,x)G_{a'b'}(y,x)\right)+\cdots. \tag{24}$$

[3]Besides the dynamical field degrees of freedom ϕ and G we will introduce a number of quantities which are (resummed) functions of these fields. These functions will be denoted by either boldface or Greek letters in the following.

The function $\mathbf{I}(x,y;G)$ is defined by

$$\mathbf{I}(x,y;G)=\frac{\lambda}{6N}G_{ab}(x,y)G_{ab}(x,y)-i\frac{\lambda}{6N}\int_z\mathbf{I}(x,z;G)G_{ab}(z,y)G_{ab}(z,y), \tag{25}$$

and resums the infinite chain of ''bubble'' graphs, which can be seen by re-expanding the series. The functions $\mathbf{I}(x,y;G)$ and the inverse of $\mathbf{B}(x,y;G)$ are closely related by

$$\mathbf{B}^{-1}(x,y;G)=\delta_{\mathcal{C}}(x-y)-i\mathbf{I}(x,y;G), \tag{26}$$

which follows from convoluting Eq. (23) with $\mathbf{B}^{-1}$ and using Eq. (25). We note that $\mathbf{B}$ and $\mathbf{I}$ do not depend on ϕ, and $\Gamma_2[\phi,G]$ is only quadratic in ϕ at NLO. Hence, the complete effective action at NLO contains only quadratic and quartic terms in ϕ.

V. THE EQUATIONS OF MOTION

From the 2PI effective action $\Gamma[\phi,G]$ at NLO we find equations of motion for the macroscopic fields ϕ and G, as indicated in Sec. II. The equation for the field expectation value (8) reads at NLO

$$-\left(\Box_x+m^2+\frac{\lambda}{6N}[\phi^2(x)+G_{cc}(x,x)]\right)\phi_a(x)=\mathbf{K}_a(x,x). \tag{27}$$

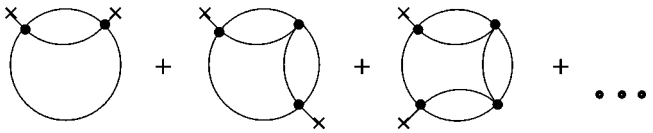

FIG. 5. NLO ϕ-dependent contribution to the 2PI effective action. Each diagram in the infinite series can be obtained from the previous one by introducing another ''rung'' with two propagator lines at each vertex. The resummed series is given by the second term in Eq. (22). The complete NLO contribution is given by the sum of the diagrams in Figs. 4 and 5.

We have written the LO contribution of the evolution equation on the LHS and combined the NLO contribution as[4]

$$\mathbf{K}_a(x,y) \equiv \mathbf{K}_a(x,y;\phi,G) \equiv \frac{\lambda}{3N}\int_z \mathbf{B}^{-1}(x,z;G)G_{ab}(y,z)\phi_b(z), \quad (28)$$

evaluated at $x=y$. We have written $\mathbf{K}_a(x,y)$ as a function of x and y for later convenience.

Equation (10) for $G_{ab}^{-1}(x,y)$ can be completed using Eq. (11) for the self-energy. The LO contribution is simply

$$\Sigma_{ab}^{\mathrm{LO}}(x,y) = -i\frac{\lambda}{6N}G_{cc}(x,x)\delta_{ab}\delta_{\mathcal{C}}(x-y). \quad (29)$$

To obtain the NLO contribution the following identity may be helpful

$$\frac{\delta \mathbf{I}(u,v;G)}{\delta G_{ab}(x,y)} = i\frac{\delta \mathbf{B}^{-1}(u,v;G)}{\delta G_{ab}(x,y)} = \frac{\lambda}{3N}\mathbf{B}^{-1}(u,x;G)G_{ab}(x,y)\mathbf{B}^{-1}(y,v;G), \quad (30)$$

where we used that

$$\frac{\delta \mathbf{B}(u,v;G)}{\delta G_{ab}(x,y)} = i\frac{\lambda}{3N}G_{ab}(x,y)\delta_{\mathcal{C}}(u-x)\delta_{\mathcal{C}}(v-y). \quad (31)$$

Collecting all the pieces, we find that Eq. (10) for the inverse propagator can be written as

$$iG_{ab}^{-1}(x,y) = -\left(\Box_x + m^2 + \frac{\lambda}{6N}[\phi^2(x)+G_{cc}(x,x)]\right)\delta_{ab}\delta_{\mathcal{C}}(x-y) - \frac{\lambda}{3N}\mathbf{B}^{-1}(x,y;G)\phi_a(x)\phi_b(y) + i\mathbf{D}(x,y)G_{ab}(x,y), \quad (32)$$

with the definition

$$\mathbf{D}(x,y) \equiv \mathbf{D}(x,y;\phi,G) \equiv i\frac{\lambda}{3N}\mathbf{B}^{-1}(x,y;G) + \left(\frac{\lambda}{3N}\right)^2\int_{uv}\mathbf{B}^{-1}(x,u;G)\phi_a(u) \times G_{ab}(u,v)\phi_b(v)\mathbf{B}^{-1}(v,y;G). \quad (33)$$

Since $\mathbf{B}^{-1}$ is of order one and $\mathbf{D}$ of order $1/N$, the second line on the RHS of Eq. (32) corresponds to the LO and the third line to the NLO contribution.

[4]Note that the classical inverse propagator iG_0^{-1} contains a LO and a NLO part.

Equations (27) and (32) together with Eqs. (28), (33) and (25), (26) form the complete set of equations which have to be solved to obtain the 2PI effective action at NLO in the $1/N$ expansion. From $\Gamma[\phi,G]$ all correlation functions can then be found by derivatives with respect to the fields as functions of the known ϕ and G. We stress that the $1/N$ expansion of the 2PI effective action is done on the level of the effective action. There are no further approximations involved on the level of the evolution equations.

We note that Eq. (33) contains a double integration over the time contour $\mathcal{C}$ which can be inconvenient for numerical purposes. It turns out that it is possible to disentangle the nested integrations by exploiting the function $\mathbf{K}_a$. Convoluting the functions $\mathbf{B}$ and $\mathbf{D}$ and using the definitions for $\mathbf{B}$ and $\mathbf{K}_a$ in Eqs. (23) and (28), one obtains

$$\mathbf{D}(x,y) = i\frac{\lambda}{3N}\delta_{\mathcal{C}}(x-y) + \frac{\lambda}{3N}\mathbf{K}_a(y,x)\phi_a(x) - i\frac{\lambda}{6N}\int_z G_{ab}(x,z)G_{ab}(x,z)\mathbf{D}(z,y). \quad (34)$$

We observe that the nested integrals have disappeared in Eq. (34) without any problems. In Appendix B we work out more details for the equations preserving the nested-integral structure. It is also convenient to rewrite Eq. (28) for $\mathbf{K}_a$ such that $\mathbf{B}$ does not appear. By convoluting $\mathbf{B}$ and $\mathbf{K}_a$, one obtains

$$\mathbf{K}_a(x,y) = \frac{\lambda}{3N}\phi_b(x)G_{ba}(x,y) - i\frac{\lambda}{6N}\int_z G_{bc}(x,z)G_{bc}(x,z)\mathbf{K}_a(z,y). \quad (35)$$

As a result, we find that $\mathbf{B}$ and $\mathbf{B}^{-1}$ are eliminated completely from the coupled equations. We also see that the gap equations for $\mathbf{D}$ and $\mathbf{K}_a$ are local in one time variable (here y), which is useful for numerical implementation.

The form of the equation of motion for the inverse propagator, Eq. (32), is suitable for a boundary value problem and can be used, in particular, to discuss the propagator in thermal equilibrium by specifying the contour $\mathcal{C}$ to the Matsubara contour along the imaginary-time axis. However, to deal with nonequilibrium time evolution, i.e., an initial value problem, the form already given in Eq. (13) is more useful. At NLO we find that the partial differential equation for the propagator takes the form

$$-\left(\Box_x + m^2 + \frac{\lambda}{6N}[\phi^2(x)+G_{cc}(x,x)]\right)G_{ab}(x,y) = i\delta_{ab}\delta_{\mathcal{C}}(x-y) + \phi_a(x)\mathbf{K}_b(x,y) - i\int_z \mathbf{D}(x,z)G_{ac}(x,z)G_{cb}(z,y). \quad (36)$$

To summarize, Eqs. (27), (36) together with Eqs. (34), (35) form the complete set of equations which have to be solved. They are completely equivalent to our first set containing Eq. (32) for the inverse propagator.

VI. THE AUXILIARY-FIELD METHOD

In this section we show that the equations derived in the previous sections can also be obtained in the auxiliary-field formulation. In particular, we discuss the difference between the $1/N$ expansion of the 2PI effective action and the ''bare-vertex approximation'' introduced in Ref. [21].

Following Refs. [21,22] we rewrite the action by introducing an auxiliary field χ as

$$S[\varphi,\chi]=-\int_x\left[\frac{1}{2}\varphi_a(\Box+m^2)\varphi_a-\frac{3N}{2\lambda}\chi^2+\frac{1}{2}\chi\varphi_a\varphi_a\right]. \tag{37}$$

Integrating out χ yields the original action (1). From the Heisenberg equations of motion we see that the auxiliary field represents the composite operator $\chi(x)=\lambda/(6N)\varphi_a(x)\varphi_a(x)$. The following one- and two-point functions can be written down:

$$\phi_a(x)=\langle\varphi_a(x)\rangle,\quad \overline{\chi}(x)=\langle\chi(x)\rangle, \tag{38}$$

and

$$\begin{aligned}G_{ab}(x,y)&=\langle T_C\varphi_a(x)\varphi_b(y)\rangle-\langle\varphi_a(x)\rangle\langle\varphi_b(y)\rangle,\\ \mathbf{K}_a(x,y)&=\langle T_C\chi(x)\varphi_a(y)\rangle-\langle\chi(x)\rangle\langle\varphi_a(y)\rangle\\ &=\overline{\mathbf{K}}_a(y,x),\\ \mathbf{D}(x,y)&=\langle T_C\chi(x)\chi(y)\rangle-\langle\chi(x)\rangle\langle\chi(y)\rangle.\end{aligned} \tag{39}$$

We note that additional ''propagators'' appear due to the introduction of the auxiliary field. Since χ is not a dynamical degree of freedom, only G_{ab} has the physical meaning of a propagator. The role of the other one- and two-point functions is to implicitly perform infinite resummations, which were carried out explicitly in the direct method in the previous sections.

Following [21] the quantum fields are combined in an extended field with $N+1$ components,

$$\Phi_i=\begin{pmatrix}\varphi_a\\ \chi\end{pmatrix}, \tag{40}$$

where $i=1,\ldots,N+1$. One may now formulate the 2PI effective action for this quantum field theory by coupling sources to the field $\Phi_i(x)$ and the bilocal field $\Phi_i(x)\Phi_j(y)$ [21]. We would like to point out that in the presence of sources the original quantum theory and the one with the auxiliary field are potentially different. For instance, in the second formalism one may differentiate with respect to the bilocal source and obtain correlation functions of $\chi(x)\varphi_a(y)$. This possibility is not present in the original theory. However, as we will see below, on the level of the equations of motion in the $1/N$ expansion of the 2PI effective action at NLO, the two approaches yield identical results.

The inverse of the classical propagator is

$$i\mathcal{G}^{-1}_{0,ij}(x,y;\overline{\Phi})=\frac{\delta^2S[\overline{\Phi}]}{\delta\overline{\Phi}_i(x)\delta\overline{\Phi}_j(y)}, \tag{41}$$

where $\overline{\Phi}_i=(\phi_a,\overline{\chi})$ and $S[\overline{\Phi}]=S[\phi,\overline{\chi}]$. It has the following components:

$$\begin{aligned}\frac{\delta^2S[\phi,\overline{\chi}]}{\delta\phi_a(x)\delta\phi_b(y)}&=-[\Box_x+m^2+\overline{\chi}(x)]\delta_{ab}\delta_C(x-y),\\ \frac{\delta^2S[\phi,\overline{\chi}]}{\delta\overline{\chi}(x)\delta\overline{\chi}(y)}&=\frac{3N}{\lambda}\delta_C(x-y),\\ \frac{\delta^2S[\phi,\overline{\chi}]}{\delta\overline{\chi}(x)\delta\phi_a(y)}&=-\phi_a(x)\delta_C(x-y).\end{aligned} \tag{42}$$

These operators are symmetric. Similarly, the matrix containing the two-point functions is defined as

$$\mathcal{G}_{ij}=\begin{pmatrix}G_{ab} & \overline{\mathbf{K}}_a\\ \mathbf{K}_b & \mathbf{D}\end{pmatrix}, \tag{43}$$

where $\overline{\mathbf{K}}_a(x,y)=\mathbf{K}_a(y,x)$ [21]. Hence, this matrix is also symmetric.

The 2PI effective action can now be written down and reads

$$\Gamma[\overline{\Phi},\mathcal{G}]=S[\overline{\Phi}]+\frac{i}{2}\mathrm{Tr}\ln\mathcal{G}^{-1}+\frac{i}{2}\mathrm{Tr}\,\mathcal{G}_0^{-1}\mathcal{G}+\Gamma_2[\mathcal{G}]+\text{const.} \tag{44}$$

Here Γ_2 is given by all two-particle irreducible graphs made with lines representing the ''propagators'' G_{ab}, $\mathbf{K}_a$, $\overline{\mathbf{K}}_a$, and $\mathbf{D}$, and the vertex $-\frac{1}{2}\chi(x)\varphi_a(x)\varphi_a(x)$. In the auxiliary-field formalism, Γ_2 does not depend on the expectation value $\overline{\Phi}_i$.

The equations of motion for the field expectation values follow by variation of Γ with respect to ϕ_a and $\overline{\chi}$. We find

$$\begin{aligned}-[\Box_x+m^2+\overline{\chi}(x)]\phi_a(x)&=\frac{1}{2}[\mathbf{K}_a(x,x)+\overline{\mathbf{K}}_a(x,x)]\\ &=\mathbf{K}_a(x,x),\end{aligned} \tag{45}$$

and

$$\overline{\chi}(x)=\frac{\lambda}{6N}[\phi^2(x)+G_{cc}(x,x)]. \tag{46}$$

The equation for the two-point function follows by variation with respect to $\mathcal{G}$, which gives

$$\mathcal{G}^{-1}_{ij}=\mathcal{G}^{-1}_{0,ij}-2i\frac{\delta\Gamma_2[\mathcal{G}]}{\delta\mathcal{G}_{ij}}. \tag{47}$$

By convoluting this equation from the right with $\mathcal{G}$ and decomposing the self-energy as[5]

$$2i\frac{\delta\Gamma_2[\mathcal{G}]}{\delta\mathcal{G}_{ij}}=\begin{pmatrix}\hat{\Sigma}_{ab} & \bar{\Xi}_a\\ \Xi_b & \Pi\end{pmatrix}, \tag{48}$$

one obtains the following set of coupled equations:

$$\begin{aligned}-[\Box_x+m^2+\bar{\chi}(x)]G_{ab}(x,y)&\\ =\phi_a(x)\mathbf{K}_b(x,y)+i\delta_{ab}\delta_{\mathcal{C}}(x-y)&\\ +i\int_z[\hat{\Sigma}_{ac}(x,z)G_{cb}(z,y)+\bar{\Xi}_a(x,z)\mathbf{K}_b(z,y)],&\end{aligned} \tag{49}$$

$$\begin{aligned}\frac{3N}{\lambda}\mathbf{K}_a(x,y)=\phi_b(x)G_{ba}(x,y)+i\int_z[\Xi_b(x,z)G_{ba}(z,y)&\\ +\Pi(x,z)\mathbf{K}_a(z,y)],&\end{aligned} \tag{50}$$

$$\begin{aligned}\frac{3N}{\lambda}\mathbf{D}(x,y)&\\ =\phi_a(x)\bar{\mathbf{K}}_a(x,y)+i\delta_{\mathcal{C}}(x-y)&\\ +i\int_z[\Xi_a(x,z)\bar{\mathbf{K}}_a(z,y)+\Pi(x,z)\mathbf{D}(z,y)],&\end{aligned} \tag{51}$$

$$\begin{aligned}-[\Box_x+m^2+\bar{\chi}(x)]\bar{\mathbf{K}}_a(x,y)=\phi_a(x)\mathbf{D}(x,y)&\\ +i\int_z[\hat{\Sigma}_{ab}(x,z)\bar{\mathbf{K}}_b(z,y)&\\ +\bar{\Xi}_a(x,z)\mathbf{D}(z,y)].&\end{aligned} \tag{52}$$

We note that Eq. (52) for $\bar{\mathbf{K}}_a$ is not an independent equation since $\bar{\mathbf{K}}_a(x,y)=\mathbf{K}_a(y,x)$. Therefore, Eq. (52) is not needed in practice.

To find explicitly at which order in the $1/N$ expansion of the 2PI effective action specific diagrams contribute, we note that in the auxiliary-field formalism the possible irreducible $O(N)$ singlets are of the form

$$\mathrm{tr}(G^n),\quad \mathbf{D},\quad \mathrm{tr}(\mathbf{K}G^n\bar{\mathbf{K}}), \tag{53}$$

with $n\geqslant 1$. From Eq. (51) it follows that $\mathbf{D}\sim 1/N$, and from Eq. (50) we find that

$$\mathrm{tr}(\mathbf{K}G^n\bar{\mathbf{K}})\sim\frac{1}{N^2}\mathrm{tr}(\phi\phi G^{n+2}) \tag{54}$$

is proportional to $1/N$ as well. Using this scaling behavior it is straightforward to give the diagrams that contribute at NLO and NNLO in the $1/N$ expansion of the 2PI effective action in the auxiliary-field formalism.

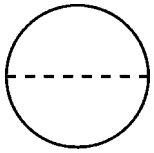

FIG. 6. NLO contribution in the $1/N$ expansion of the 2PI effective action in the auxiliary-field formalism. The full line denotes the scalar propagator G_{ab}, the dashed line the auxiliary-field propagator $\mathbf{D}$.

We find that the NLO contribution to Γ_2 consists of one graph only,

$$\Gamma_2^{\mathrm{NLO}}[\mathcal{G}]=\frac{i}{4}\int_{xy}G_{ab}(x,y)G_{ab}(x,y)\mathbf{D}(x,y), \tag{55}$$

shown in Fig. 6. From this expression the self-energies defined above follow:

$$\begin{aligned}\hat{\Sigma}_{ab}^{\mathrm{NLO}}(x,y)&=-G_{ab}(x,y)\mathbf{D}(x,y),\\ \Pi^{\mathrm{NLO}}(x,y)&=-\frac{1}{2}G_{ab}(x,y)G_{ab}(x,y),\\ \Xi_a^{\mathrm{NLO}}(x,y)&=0.\end{aligned} \tag{56}$$

Inserting these expressions in Eqs. (49)–(51), we immediately recover our final result at NLO, Eqs. (27), (34–36), obtained by the direct method in Sec. V.[6]

Only three diagrams contribute in the auxiliary-field formulation at NNLO. They are shown in Fig. 7. We note that diagrams with the mixed propagator $\mathbf{K}_a$ (resulting in a nonvanishing Ξ_a and $\bar{\Xi}_a$) appear only at NNLO. In Ref. [21] the first NNLO diagram,

$$\Gamma_2^{\mathrm{NNLOa}}[\mathcal{G}]=\frac{i}{2}\int_{xy}\mathbf{K}_a(x,y)G_{ab}(x,y)\bar{\mathbf{K}}_b(x,y), \tag{57}$$

was combined with the NLO diagram of Fig. 6 in the so-called bare-vertex approximation (BVA). We conclude that in the presence of a field expectation value the BVA approximation is not consistent with the $1/N$ approximation of the 2PI effective action discussed here. For vanishing ϕ, the $1/N$ approximation of the 2PI effective action at NLO and the BVA ansatz are identical.[7]

[5]Note that in the auxiliary-field formalism $\hat{\Sigma}_{ab}$ does not receive a local LO contribution. It differs therefore from the self-energy Σ_{ab} in the direct method, obtained by varying $\Gamma_2[\phi,G]$.

[6]Therefore, we use the same notation for the functions $\mathbf{K}$, $\mathbf{D}$ and Π in Secs. V to VII.

[7]For similar approximation schemes see also Ref. [23].

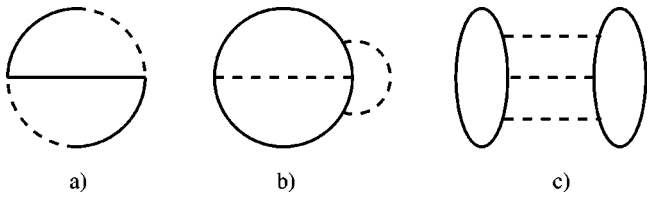

FIG. 7. NNLO contribution in the $1/N$ expansion of the 2PI effective action in the auxiliary-field formalism. The full-dashed lines denote the mixed propagators $\mathbf{K}_a$, $\overline{\mathbf{K}}_a$.

VII. EVOLUTION EQUATIONS FOR THE SPECTRAL AND STATISTICAL FUNCTIONS AT NLO

In order to describe nonequilibrium dynamics we will now specify the contour $\mathcal{C}$ to the standard Schwinger-Keldysh contour along the real-time axis [24].[8] The two-point function can be decomposed as

$$G_{ab}(x,y)=G^{>}_{ab}(x,y)\Theta_{\mathcal{C}}(x^0-y^0)+G^{<}_{ab}(x,y)\Theta_{\mathcal{C}}(y^0-x^0), \tag{58}$$

where $G^{>}_{ab}(x,y)=G^{<}_{ab}{}^{*}(x,y)$ are complex functions. For the real scalar field theory it is convenient to express the evolution equations in terms of two independent real-valued two-point functions, which can be associated to the expectation values of the commutator and the anti-commutator of two fields [4,5,8]. We define

$$F_{ab}(x,y)=\frac{1}{2}(G^{>}_{ab}(x,y)+G^{<}_{ab}(x,y))=\mathrm{Re}[G^{>}_{ab}(x,y)], \tag{59}$$

$$\rho_{ab}(x,y)=i(G^{>}_{ab}(x,y)-G^{<}_{ab}(x,y))=-2\,\mathrm{Im}[G^{>}_{ab}(x,y)]. \tag{60}$$

Here F is the statistical propagator and ρ denotes the spectral function, with the properties $F^{*}_{ab}(x,y)=F_{ab}(x,y)=F_{ba}(y,x)$ and $\rho^{*}_{ab}(x,y)=\rho_{ab}(x,y)=-\rho_{ba}(y,x)$.

In order to proceed it is convenient to separate the singular part of $\mathbf{D}$ [see Eq. (34)] and write

$$\mathbf{D}(x,y)=\frac{\lambda}{3N}[i\,\delta_{\mathcal{C}}(x-y)+\hat{\mathbf{D}}(x,y)], \tag{61}$$

with

$$\hat{\mathbf{D}}(x,y)=\mathbf{K}_a(y,x)\,\phi_a(x)-\frac{\lambda}{3N}\Pi(x,y)+\frac{i\lambda}{3N}\int_z\Pi(x,z)\hat{\mathbf{D}}(z,y). \tag{62}$$

For the functions $\mathbf{K}_a(x,y)$ [see Eq. (35)] and $\hat{\mathbf{D}}(x,y)$ we define the statistical and spectral components as

$$\mathbf{K}^F_a(x,y)=\frac{1}{2}(\mathbf{K}^{>}_a(x,y)+\mathbf{K}^{<}_a(x,y))=\mathrm{Re}[\mathbf{K}^{>}_a(x,y)], \tag{63}$$

$$\mathbf{K}^\rho_a(x,y)=i(\mathbf{K}^{>}_a(x,y)-\mathbf{K}^{<}_a(x,y))=-2\,\mathrm{Im}[\mathbf{K}^{>}_a(x,y)], \tag{64}$$

and the same for $\hat{\mathbf{D}}_F(x,y)$ and $\hat{\mathbf{D}}_\rho(x,y)$.

Now we have all the necessary definitions and relations to express the time evolution equations for the field expectation value and Green's function along the Schwinger-Keldysh contour as real and causal equations. The time evolution equation for the field reads

$$-[\Box_x+m^2+\overline{\chi}(x)]\phi_a(x)=\mathbf{K}^F_a(x,x) \tag{65}$$

with

$$\overline{\chi}(x)=\frac{\lambda}{6N}[\phi^2(x)+F_{cc}(x,x)]. \tag{66}$$

The functions $\mathbf{K}^F_a$ and $\mathbf{K}^\rho_a$ satisfy the equations

$$\mathbf{K}^F_a(x,y)=\frac{\lambda}{3N}\phi_b(x)F_{ba}(x,y)+\frac{\lambda}{3N}\int_0^{x^0}dz\,\Pi_\rho(x,z)\mathbf{K}^F_a(z,y)-\frac{\lambda}{3N}\int_0^{y^0}dz\,\Pi_F(x,z)\mathbf{K}^\rho_a(z,y), \tag{67}$$

$$\mathbf{K}^\rho_a(x,y)=\frac{\lambda}{3N}\phi_b(x)\rho_{ba}(x,y)+\frac{\lambda}{3N}\int_{y^0}^{x^0}dz\,\Pi_\rho(x,z)\mathbf{K}^\rho_a(z,y),$$

where we employ the notation

$$\int_0^{x^0}dz\equiv\int_0^{x^0}dz^0\int d\mathbf{z}, \tag{68}$$

and

$$\Pi_F(x,y)=-\frac{1}{2}\left[F_{ab}(x,y)F_{ab}(x,y)-\frac{1}{4}\rho_{ab}(x,y)\rho_{ab}(x,y)\right],$$

$$\Pi_\rho(x,y)=-F_{ab}(x,y)\rho_{ab}(x,y). \tag{69}$$

The statistical propagator obeys

$$\begin{aligned}-[\Box_x+m^2+\overline{\chi}(x)]F_{ab}(x,y)&=\frac{\lambda}{3N}F_{ac}(x,x)F_{cb}(x,y)+\phi_a(x)\mathbf{K}^F_b(x,y)\\&\quad+\int_0^{x^0}dz\,\hat{\Sigma}^\rho_{ac}(x,z)F_{cb}(z,y)\\&\quad-\int_0^{y^0}dz\,\hat{\Sigma}^F_{ac}(x,z)\rho_{cb}(z,y),\end{aligned} \tag{70}$$

and the spectral function

[8]We use a Gaussian initial density matrix. Non-Gaussian initial density matrices are also possible, see e.g. Refs. [7,10].

$$-[\Box_x+m^2+\overline{\chi}(x)]\rho_{ab}(x,y)$$
$$=\frac{\lambda}{3N}F_{ac}(x,x)\rho_{cb}(x,y)+\phi_a(x)\mathbf{K}^\rho_b(x,y)$$
$$+\int_{y^0}^{x^0}dz\,\hat{\Sigma}^\rho_{ac}(x,z)\rho_{cb}(z,y). \tag{71}$$

Here we use the notation

$$\hat{\Sigma}^F_{ab}(x,y)=-\frac{\lambda}{3N}\left[F_{ab}(x,y)\hat{\mathbf{D}}_F(x,y)-\frac{1}{4}\rho_{ab}(x,y)\hat{\mathbf{D}}_\rho(x,y)\right], \tag{72}$$

$$\hat{\Sigma}^\rho_{ab}(x,y)=-\frac{\lambda}{3N}[\rho_{ab}(x,y)\hat{\mathbf{D}}_F(x,y)+F_{ab}(x,y)\hat{\mathbf{D}}_\rho(x,y)], \tag{73}$$

with

$$\hat{\mathbf{D}}_F(x,y)=\mathbf{K}^F_a(y,x)\phi_a(x)-\frac{\lambda}{3N}\Pi_F(x,y)$$
$$+\frac{\lambda}{3N}\int_0^{x^0}dz\,\Pi_\rho(x,z)\hat{\mathbf{D}}_F(z,y)$$
$$-\frac{\lambda}{3N}\int_0^{y^0}dz\,\Pi_F(x,z)\hat{\mathbf{D}}_\rho(z,y),$$

$$\hat{\mathbf{D}}_\rho(x,y)=-\mathbf{K}^\rho_a(y,x)\phi_a(x)-\frac{\lambda}{3N}\Pi_\rho(x,y)$$
$$+\frac{\lambda}{3N}\int_{y^0}^{x^0}dz\,\Pi_\rho(x,z)\hat{\mathbf{D}}_\rho(z,y). \tag{74}$$

In the absence of a field-expectation value ($\phi_a=0$) we find that $\mathbf{K}^F_a=\mathbf{K}^\rho_a=0$ and the equations above reduce to those treated in [4,5] for diagonal two-point functions.

In order to completely determine the time evolution, Eqs. (65), (70) and (71) have to be implemented with initial conditions taken at $x^0=y^0=0$. For the field $\phi_a(x)$ one may choose nonvanishing values $\phi_a(x^0=0,\mathbf{x})$, but vanishing "velocities" $\partial_{x^0}\phi_a(x)|_{x^0=0}=0$. The initial values for the spectral function are completely fixed by the equal-time properties [8]

$$\rho_{ab}(x,y)|_{x^0=y^0}=0,$$
$$\partial_{x^0}\rho_{ab}(x,y)|_{x^0=y^0}=\delta_{ab}\delta^d(\mathbf{x}-\mathbf{y}). \tag{75}$$

Nontrivial information about the initial density matrix is contained in (derivatives of) the statistical two-point function at initial time

$$F_{ab}(x,y)|_{x^0=y^0=0},\quad \partial_{x^0}F_{ab}(x,y)|_{x^0=y^0=0},$$
$$\partial_{x^0}\partial_{y^0}F_{ab}(x,y)|_{x^0=y^0=0}. \tag{76}$$

Specification of these three functions is necessary and sufficient to solve the equations of motion.

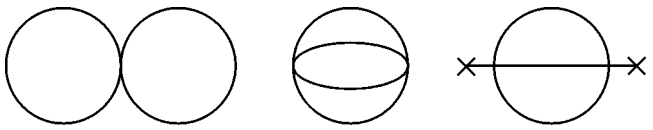

FIG. 8. Diagrams contributing in the $1/N$ expansion of the 2PI effective action when an additional weak-coupling expansion to second order in λ is performed.

VIII. WEAK COUPLING EXPANSION

In order to simplify the interrelated set of nonperturbative NLO equations of motion given in the previous section, we discuss here a truncated version of the $1/N$ approximation of the 2PI effective action for the case that the coupling is weak. It amounts to expanding the effective action to second order in explicit factors of the coupling constant λ. Since $\Gamma_2^{\rm LO}$ is proportional to λ it is preserved completely. For the NLO contribution $\Gamma_2^{\rm NLO}$ in Eq. (22) we find

$$\Gamma_2^{\rm NLO}[\phi,G]\simeq\frac{\lambda}{6N}\int_x\Pi(x,x)+i\left(\frac{\lambda}{6N}\right)^2\int_{xy}\Pi(x,y)\Pi(x,y)$$
$$-2i\left(\frac{\lambda}{6N}\right)^2\int_{xy}\Pi(x,y)\phi_a(x)G_{ab}(x,y)\phi_b(y), \tag{77}$$

where we use again the notation $\Pi(x,y)=-\frac{1}{2}G_{ab}(x,y)G_{ab}(x,y)$. The corresponding diagrams are presented in Fig. 8.[9]

The weak-coupling expansion affects the equations of motion through the auxiliary variables $\mathbf{K}_a$ and $\hat{\mathbf{D}}$,

$$\mathbf{K}_a(x,y)\simeq\frac{\lambda}{3N}\phi_b(x)G_{ba}(x,y)$$
$$+i\left(\frac{\lambda}{3N}\right)^2\int_z\Pi(x,z)\phi_b(z)G_{ba}(z,y),$$

$$\hat{\mathbf{D}}(x,y)\simeq\frac{\lambda}{3N}[\phi_a(x)G_{ab}(x,y)\phi_b(y)-\Pi(x,y)]. \tag{78}$$

In the evolution equations (70) and (71) for the statistical and spectral function Eq. (67) is replaced by

[9]Here we consider the simple case of a field expectation value for which $(\lambda/6N)\phi^2$ is small compared to the characteristic mass scale. We stress that for a consistent weak coupling expansion it is important to note that a nonzero minimum at $\phi^2=\phi_0^2$ of the classical potential in Eq. (1) scales as $\phi_0^2=-(6N/\lambda)m^2$. Therefore, in a situation with spontaneously broken symmetry it is not sufficient to count only the powers of λ coming from the vertices, as exemplified in this section. A consistent $\mathcal{O}(\lambda)$ scheme would have to take into account the first and the third graph of Fig. 8, while at $\mathcal{O}(\lambda^2)$ the three-loop graphs of Figs. 8 and 5 would have to be taken into account.

$$\mathbf{K}_a^F(x,y) \simeq \frac{\lambda}{3N}\phi_b(x)F_{ba}(x,y) + \left(\frac{\lambda}{3N}\right)^2 \int_0^{x^0} dz\, \Pi_\rho(x,z)\phi_b(z)F_{ba}(z,y) - \left(\frac{\lambda}{3N}\right)^2 \int_0^{y^0} dz\, \Pi_F(x,z)\phi_b(z)\rho_{ba}(z,y), \tag{79}$$

$$\mathbf{K}_a^\rho(x,y) \simeq \frac{\lambda}{3N}\phi_b(x)\rho_{ba}(x,y) + \left(\frac{\lambda}{3N}\right)^2 \int_{y^0}^{x^0} dz\, \Pi_\rho(x,z)\phi_b(z)\rho_{ba}(z,y),$$

and Eq. (74) simplifies considerably to

$$\hat{\mathbf{D}}_F(x,y) \simeq \frac{\lambda}{3N}[\phi_a(x)F_{ab}(x,y)\phi_b(y) - \Pi_F(x,y)],$$

$$\hat{\mathbf{D}}_\rho(x,y) \simeq \frac{\lambda}{3N}[\phi_a(x)\rho_{ab}(x,y)\phi_b(y) - \Pi_\rho(x,y)]. \tag{80}$$

IX. SUMMARY

We have derived the 2PI effective action $\Gamma[\phi,G]$ for the $O(N)$ model using the $1/N$ expansion of the 2PI effective action to next-to-leading order. A detailed discussion of the classification of diagrams was presented. The equations of motion for the field expectation value ϕ and the two-point function G were calculated without further approximations. We showed the equivalence of the direct calculation with the auxiliary-field formulation.

A detailed, but separate investigation would be necessary in order to discuss the question of the nonperturbative renormalizability of $\Gamma[\phi,G]$ and the evolution equations derived above within the approximations considered in this paper. In principle, this problem may be treated following methods outlined in Ref. [12]. However, concerning the applications we have in mind and which are listed in the Introduction, we emphasize that the physics of these problems is dominated by soft excitations and requires a finite cutoff. Therefore, from the practical point of view the important next step is to solve these equations along the lines of Refs. [4,5] using a straightforward lattice discretization.

ACKNOWLEDGMENTS

J.B. thanks Jörn Knoll and Hendrik van Hees for interesting discussions. G.A. was supported by the U. S. Department of Energy under Contract No. DE-FG02-01ER41190. D.A. is supported by DFG, project FOR 339/2-1.

APPENDIX A

In this section we discuss possible further approximations consistent with an expansion in powers of $1/N$ and comment on some aspects of Goldstone's theorem. We note that within the NLO approximation the replacement

$$\mathrm{tr}\, G^2 \to (\mathrm{tr}\, G)^2/N \tag{A1}$$

in the expressions for the diagrams discussed in Sec. III is correct up to higher order terms. This corresponds to the replacement $G_{ab}(x,y)G_{ab}(x,y) \to [G_{aa}(x,y)]^2/N$ in the functions $\mathbf{B}(G)$ of Eq. (23) and $\mathbf{I}(G)$ of Eq. (25). One observes that the resulting expressions can no longer be represented by the diagrams of Sec. III. To verify this replacement up to NNLO corrections we note that (for given space-time coordinates) G can be diagonalized by virtue of $O(N)$ rotations. In particular, G is diagonal up to subleading corrections. This can be seen explicitly from the LO solution of Eq. (9) for the propagator, $G_{ab}^{(\mathrm{LO})} \sim \delta_{ab}$, which follows from the fact that the LO diagrams depend only on the invariants $\mathrm{tr}\, G$ and ϕ^2 (cf. Sec. III). Since the invariant $\mathrm{tr}\, G^2$ does not appear in LO diagrams, the replacement (A1) is correct within the NLO approximation. We stress here that Eq. (A1) has not been used in the derivation of any equation presented in this paper.

A similar argument cannot be applied to the invariant $\mathrm{tr}(\phi\phi G) = \phi_a G_{ab}\phi_b$. To see this, it is sufficient to restrict our attention to constant field configurations. In this case, it follows from $O(N)$ symmetry that the most general form of the propagator is

$$G_{ab}^{(\mathrm{stat})}(\phi) = G_L(\phi^2)P_{ab}^L + G_T(\phi^2)P_{ab}^T, \tag{A2}$$

where $P_{ab}^L = \phi_a\phi_b/\phi^2$ and $P_{ab}^T = \delta_{ab} - P_{ab}^L$ are respectively the longitudinal and transverse projectors with respect to the field direction. Using this decomposition, we first check that the replacement (A1) is valid at NLO, in agreement with the above general discussion. Indeed the difference

$$\mathrm{tr}\, G^2 - \frac{(\mathrm{tr}\, G)^2}{N} = (G_L - G_T)^2\left(1 - \frac{1}{N}\right) \sim N^0 \tag{A3}$$

is subleading (recall that $\mathrm{tr}\, G^2 \sim \mathrm{tr}\, G \sim N$). However,

$$\mathrm{tr}(\phi\phi G) - \frac{\phi^2 \mathrm{tr}\, G}{N} = \phi^2(G_L - G_T)\left(1 - \frac{1}{N}\right) \sim N \tag{A4}$$

demonstrates that $\mathrm{tr}(\phi\phi G)$ cannot be replaced by $\phi^2 \mathrm{tr}\, G/N$ up to higher order corrections.

In the remainder of this appendix we want to show that Goldstone's theorem is satisfied at any order in the $1/N$ expansion of the 2PI effective action. Following Sec. III the 2PI effective action can be written as a function of the $O(N)$ invariants (15) only,

$$\Gamma[\phi,G] \equiv \Gamma[\phi^2, \mathrm{tr}(G^n), \mathrm{tr}(\phi\phi G^p)]. \tag{A5}$$

In the case of spontaneous symmetry breaking one has a constant $\phi \neq 0$ and the propagator can be parametrized as in Eq. (A2). The standard 1PI effective action $\Gamma_{1PI}[\phi]$ is obtained by evaluating the 2PI effective action at the stationary value (9) for G [3], and the mass matrix $\mathcal{M}_{ab}$ can then be obtained from

$$\mathcal{M}_{ab} \sim \left. \frac{\delta^2 \Gamma[\phi, G^{(\mathrm{stat})}(\phi)]}{\delta\phi_a \delta\phi_b} \right|_{\phi=\mathrm{const}}. \tag{A6}$$

If $\Gamma_{1PI}[\phi]$ is calculated from Eqs. (A5) and (A2) one observes that indeed the 1PI effective action depends only on one invariant, ϕ^2. The form of the mass matrix $\mathcal{M}_{ab}$ can now be inferred straightforwardly from $\Gamma_{1PI}[\phi]$. To obtain the effective potential $U(\phi^2/2)$, we write

$$\Gamma_{1PI}[\phi]\big|_{\phi=\mathrm{const}} = \Omega_{d+1} U(\phi^2/2), \tag{A7}$$

where Ω_{d+1} is the $(d+1)$-dimensional Euclidean volume. The expectation value of the field is given by the solution of the stationarity equation (7) which becomes

$$\frac{\partial U(\phi^2/2)}{\partial \phi_a} = \phi_a U' = 0, \tag{A8}$$

where $U' \equiv \partial U/\partial(\phi^2/2)$ and similarly for higher derivatives. The mass matrix reads

$$\begin{aligned} \mathcal{M}^2_{ab} &= \frac{\partial^2 U(\phi^2/2)}{\partial\phi_a \partial\phi_b} \\ &= \delta_{ab} U' + \phi_a \phi_b U'' \\ &= (U' + \phi^2 U'') P^L_{ab} + U' P^T_{ab}. \end{aligned} \tag{A9}$$

In the symmetric phase ($\phi_a = 0$) one finds that all modes have equal mass squared $\mathcal{M}^2_{ab} = U' \delta_{ab}$. In the broken phase, with $\phi_a \neq 0$, Eq. (A8) implies that the mass of the transverse modes $\sim U'$ vanishes identically in agreement with Goldstone's theorem. For a similar discussion, see Ref. [25]. Truncations of the 2PI effective action may not show manifestly the presence of massless transverse modes if one considers the solution $G^{(\mathrm{stat})}$ of Eq. (9) instead of the second variation of $\Gamma[\phi, G^{(\mathrm{stat})}]$ for constant fields. For an early discussion of this point see Ref. [26] as well as the comments in Ref. [12].

APPENDIX B

In this appendix we present the equations for the statistical and spectral functions preserving the nested integral structure and keeping the "chain of bubbles" $\mathbf{I}(x,y;G)$ as the basic quantity.

All local contributions can be combined in an effective mass parameter

$$M^2_{ab}(x) = [m^2 + \overline{\chi}(x)]\delta_{ab} + \frac{\lambda}{3N}[\phi_a(x)\phi_b(x) + G_{ab}(x,x)], \tag{B1}$$

and Eq. (13) can be written as

$$\begin{aligned} &-[\Box_x \delta_{ac} + M^2_{ac}(x)] G_{cb}(x,y) \\ &\quad = i\delta_{ab}\delta_C(x-y) + i\int_z \Sigma_{ac}(x,z) G_{cb}(z,y), \end{aligned} \tag{B2}$$

with the "nonlocal" self-energy at NLO (we suppress the G dependence)

$$\begin{aligned} \Sigma_{ab}(x,y) = -\frac{\lambda}{3N}\{&\mathbf{I}(x,y)[\phi_a(x)\phi_b(y) + G_{ab}(x,y)] \\ &+ \mathbf{P}(x,y) G_{ab}(x,y)\}. \end{aligned} \tag{B3}$$

Here we defined

$$\mathbf{P}(x,y) = -\frac{\lambda}{3N}\int_{uv} \mathbf{B}^{-1}(x,u)\Delta(u,v)\mathbf{B}^{-1}(v,y), \tag{B4}$$

$$\Delta(x,y) = -\phi_a(x) G_{ab}(x,y)\phi_b(y). \tag{B5}$$

Eq. (B2) results in the standard time evolution equations for F and ρ [8]

$$\begin{aligned} [\Box_x \delta_{ac} + M^2_{ac}(x)] F_{cb}(x,y) = &-\int_0^{x^0} dz\, \Sigma^\rho_{ac}(x,z) F_{cb}(z,y) \\ &+ \int_0^{y^0} dz\, \Sigma^F_{ac}(x,z)\rho_{cb}(z,y), \end{aligned} \tag{B6}$$

$$[\Box_x \delta_{ac} + M^2_{ac}(x)]\rho_{cb}(x,y) = -\int_{y^0}^{x^0} dz\, \Sigma^\rho_{ac}(x,z)\rho_{cb}(z,y), \tag{B7}$$

with

$$M^2_{ab}(x) = [m^2 + \overline{\chi}(x)]\delta_{ab} + \frac{\lambda}{3N}[\phi_a(x)\phi_b(x) + F_{ab}(x,x)], \tag{B8}$$

and the nonlocal self-energies

$$\begin{aligned} \Sigma^F_{ab}(x,y) = -\frac{\lambda}{3N}\Big\{&\mathbf{I}_F(x,y)[\phi_a(x)\phi_b(y) + F_{ab}(x,y)] \\ &- \frac{1}{4}\mathbf{I}_\rho(x,y)\rho_{ab}(x,y) + \mathbf{P}_F(x,y)F_{ab}(x,y) \\ &- \frac{1}{4}\mathbf{P}_\rho(x,y)\rho_{ab}(x,y)\Big\}, \end{aligned} \tag{B9}$$

$$\begin{aligned} \Sigma^\rho_{ab}(x,y) = -\frac{\lambda}{3N}\{&\mathbf{I}_\rho(x,y)[\phi_a(x)\phi_b(y) + F_{ab}(x,y)] \\ &+ \mathbf{I}_F(x,y)\rho_{ab}(x,y) + \mathbf{P}_\rho(x,y)F_{ab}(x,y) \\ &+ \mathbf{P}_F(x,y)\rho_{ab}(x,y)\}. \end{aligned} \tag{B10}$$

The functions $\mathbf{I}_F$ and $\mathbf{I}_\rho$ satisfy [4]

$$\begin{aligned} \mathbf{I}_F(x,y) = &-\frac{\lambda}{3N}\Pi_F(x,y) + \frac{\lambda}{3N}\int_0^{x^0} dz\, \mathbf{I}_\rho(x,z)\Pi_F(z,y) \\ &- \frac{\lambda}{3N}\int_0^{y^0} dz\, \mathbf{I}_F(x,z)\Pi_\rho(z,y), \end{aligned}$$

$$\mathbf{I}_\rho(x,y) = -\frac{\lambda}{3N}\Pi_\rho(x,y) + \frac{\lambda}{3N}\int_{y^0}^{x^0} dz\, \mathbf{I}_\rho(x,z)\Pi_\rho(z,y), \tag{B11}$$

and the nested integrals are

$$\begin{aligned}\mathbf{P}_F(x,y) = -\frac{\lambda}{3N}\Bigg\{ & \Delta_F(x,y) - \int_0^{x^0} dz[\Delta_\rho(x,z)\mathbf{I}_F(z,y) + \mathbf{I}_\rho(x,z)\Delta_F(z,y)] + \int_0^{y^0} dz[\Delta_F(x,z)\mathbf{I}_\rho(z,y) + \mathbf{I}_F(x,z)\Delta_\rho(z,y)] \\ & - \int_0^{x^0} dz \int_0^{y^0} dv\, \mathbf{I}_\rho(x,z)\Delta_F(z,v)\mathbf{I}_\rho(v,y) + \int_0^{x^0} dz \int_0^{z^0} dv\, \mathbf{I}_\rho(x,z)\Delta_\rho(z,v)\mathbf{I}_F(v,y) \\ & + \int_0^{y^0} dz \int_{z^0}^{y^0} dv\, \mathbf{I}_F(x,z)\Delta_\rho(z,v)\mathbf{I}_\rho(v,y)\Bigg\},\end{aligned} \tag{B12}$$

and

$$\mathbf{P}_\rho(x,y) = -\frac{\lambda}{3N}\left\{ \Delta_\rho(x,y) - \int_{y^0}^{x^0} dz[\Delta_\rho(x,z)\mathbf{I}_\rho(z,y) + \mathbf{I}_\rho(x,z)\Delta_\rho(z,y)] + \int_{y^0}^{x^0} dz \int_{y^0}^{z^0} dv\, \mathbf{I}_\rho(x,z)\Delta_\rho(z,v)\mathbf{I}_\rho(v,y)\right\}, \tag{B13}$$

with $\Delta_F(x,y) = -\phi_a(x)F_{ab}(x,y)\phi_b(y)$ and $\Delta_\rho(x,y) = -\phi_a(x)\rho_{ab}(x,y)\phi_b(y)$. The RHS in Eq. (65) for the field expectation value reads

$$\mathbf{K}_a^F(x,x) = \frac{\lambda}{3N}F_{ab}(x,x)\phi_b(x) - \frac{\lambda}{3N}\int_0^{x^0} dy[\mathbf{I}_\rho(x,y)F_{ab}(x,y) + \mathbf{I}_F(x,y)\rho_{ab}(x,y)]\phi_b(y). \tag{B14}$$

Note that the nested time integrals in Eqs. (B12), (B13) have been eliminated in the equations discussed in Secs. V and VII by a convenient choice of auxiliary variables.

[1] For recent reviews, see D. Bödeker, Nucl. Phys. **B94**, 61 (2001); J.P. Blaizot and E. Iancu, Phys. Rep. **359**, 355 (2002).

[2] *Progress in Nonequilibrium Green's Functions*, Proceedings of the Conference ''Kadanoff-Baym Equations: Progress and Perspectives for Many-Body Physics,'' edited by M. Bonitz (World Scientific, Singapore, 2000); see also K.C. Chou, Z.B. Su, B.L. Hao, and L. Yu, Phys. Rep. **118**, 1 (1985).

[3] J.M. Cornwall, R. Jackiw, and E. Tomboulis, Phys. Rev. D **10**, 2428 (1974); see also J.M. Luttinger and J.C. Ward, Phys. Rev. **118**, 1417 (1960); G. Baym, *ibid.* **127**, 1391 (1962).

[4] J. Berges, Nucl. Phys. **A699**, 847 (2002).

[5] G. Aarts and J. Berges, Phys. Rev. Lett. **88**, 041603 (2002).

[6] L.M. Bettencourt and C. Wetterich, Phys. Lett. B **430**, 140 (1998); B. Mihaila, T. Athan, F. Cooper, J. Dawson, and S. Habib, Phys. Rev. D **62**, 125015 (2000).

[7] J. Berges and J. Cox, Phys. Lett. B **517**, 369 (2001).

[8] G. Aarts and J. Berges, Phys. Rev. D **64**, 105010 (2001).

[9] L. P. Kadanoff and G. Baym, *Quantum Statistical Mechanics* (Benjamin, New York, 1962).

[10] E. Calzetta and B.L. Hu, Phys. Rev. D **37**, 2878 (1988).

[11] Y.B. Ivanov, J. Knoll, and D.N. Voskresensky, Nucl. Phys. **A657**, 413 (1999).

[12] H. van Hees and J. Knoll, Phys. Rev. D **65**, 025010 (2002); **65**, 105005 (2002).

[13] J.P. Blaizot, E. Iancu, and A. Rebhan, Phys. Rev. Lett. **83**, 2906 (1999); Phys. Rev. D **63**, 065003 (2001).

[14] E. Braaten and E. Petitgirard, Phys. Rev. D **65**, 041701 (2002); **65**, 085039 (2002).

[15] Among related literature using a leading-order $1/N$ expansion, see, e.g., F. Cooper, S. Habib, Y. Kluger, E. Mottola, J.P. Paz, and P.R. Anderson, Phys. Rev. D **50**, 2848 (1994); D. Boyanovsky, H.J. de Vega, R. Holman, D.S. Lee, and A. Singh, *ibid.* **51**, 4419 (1995); D. Boyanovsky, H.J. de Vega, R. Holman, and J.F. Salgado, *ibid.* **54**, 7570 (1996); F. Cooper, S. Habib, Y. Kluger, and E. Mottola, *ibid.* **55**, 6471 (1997); J. Baacke, K. Heitmann, and C. Pätzold, *ibid.* **58**, 125013 (1998); G. Aarts and J. Smit, *ibid.* **61**, 025002 (2000), and references therein.

[16] S. Mrowczynski and B. Müller, Phys. Lett. B **363**, 1 (1995); D. Boyanovsky, H.J. de Vega, and R. Holman, Phys. Rev. D **51**, 734 (1995); K. Rajagopal, in *Quark-Gluon Plasma 2*, edited by R. Hwa (World Scientific, Singapore, 1995), p. 485; J. Randrup, Heavy Ion Phys. **9**, 289 (1999); D.I. Kaiser, Phys. Rev. D **59**, 117901 (1999); J. Serreau, *ibid.* **63**, 054003 (2001).

[17] D. Ahrensmeier, R. Baier, and M. Dirks, Phys. Lett. B **484**, 58 (2000); hep-ph/0105189.

[18] D. Kharzeev, R.D. Pisarski, and M.H. Tytgat, Phys. Rev. Lett. **81**, 512 (1998); hep-ph/0012012.

[19] J.H. Traschen and R.H. Brandenberger, Phys. Rev. D **42**, 2491 (1990); L. Kofman, A.D. Linde, and A.A. Starobinsky, Phys. Rev. Lett. **73**, 3195 (1994); Phys. Rev. D **56**, 3258 (1997).

[20] S.Y. Khlebnikov and I.I. Tkachev, Phys. Rev. Lett. **77**, 219 (1996); T. Prokopec and T.G. Roos, Phys. Rev. D **55**, 3768 (1997).

[21] B. Mihaila, F. Cooper, and J.F. Dawson, Phys. Rev. D **63**,

096003 (2001); K. Blagoev, F. Cooper, J. Dawson, and B. Mihaila, *ibid.* **64**, 125003 (2001).
[22] S.R. Coleman, R. Jackiw, and H.D. Politzer, Phys. Rev. D **10**, 2491 (1974).
[23] M. Lutz and J. Praschifka, Int. J. Mod. Phys. A **8**, 277 (1993).
[24] J. Schwinger, J. Math. Phys. **2**, 407 (1961); L.V. Keldysh, Zh. Éksp. Teor. Fiz. **47**, 1515 (1964) [Sov. Phys. JETP **20**, 1018 (1965)]; K.T. Mahanthappa, Phys. Rev. **126**, 329 (1962); P.M. Bakshi and K.T. Mahanthappa, J. Math. Phys. **4**, 1 (1963); **4**, 12 (1963).
[25] H. Verschelde and J. De Pessemier, Eur. Phys. J. C **22**, 771 (2002).
[26] G. Baym and G. Grinstein, Phys. Rev. D **15**, 2897 (1977).